International Journal of Chemical Studies

P-ISSN: 2349–8528
E-ISSN: 2321–4902
IJCS 2017; 5(4): 1489-1494

Received: 22-05-2017
Accepted: 24-06-2017

Manju Kumari Choudhary
Department of Molecular Biology and Biotechnology, Rajasthan College of Agriculture, Maharana Pratap University of Agriculture and Technology, Udaipur, Rajasthan, India

Swati
Department of Molecular Biology and Biotechnology, Rajasthan College of Agriculture, Maharana Pratap University of Agriculture and Technology, Udaipur, Rajasthan, India

Vinod Saharan
Department of Molecular Biology and Biotechnology, Rajasthan College of Agriculture, Maharana Pratap University of Agriculture and Technology, Udaipur, Rajasthan, India

Correspondence
Manju Kumari Choudhary
Department of Molecular Biology and Biotechnology, Rajasthan College of Agriculture, Maharana Pratap University of Agriculture and Technology, Udaipur, Rajasthan, India

Synthesis, characterization and evaluation of physico-chemical profile of Cu-Chitosan Nanocomposite

Manju Kumari Choudhary, Swati and Vinod Saharan

Abstract
In this paper, we have synthesized stable and monodisperse Cu-chitosan nanocomposites (NCPs) based on the ionic gelation of chitosan with tripolyphosphate anions and Copper ions. The physicochemical properties i.e. particle size (295.4 nm), polydispersity index (0.28), zeta potential (+ 19.6 mV), functional group analysis (chitosan, TPP and Cu interaction by frequency distribution), shape (sphere), morphology (highly porous), elemental composition (C,O,P,N and Cu) were characterized by Dynamic light scattering (DLS), Fourier transforms infrared (FTIR), Transmission electron microscopy (TEM), Scanning electron microscopy (SEM) and SEM energy dispersive X-ray spectroscope (SEM-EDS). Further, release profile of metal elements in Cu-chitosan NCPs was studied by atomic absorption spectroscopy (AAS) under varying pH, agitation period and agitation rate. The objective of this study was to solve the problem of preparation of Cu-chitosan NCPs with high degree of monodispersity and stability and investigate the effect of various parameters on the release profile of metal elements in Cu-chitosan NCPs.

Keywords: Cu-chitosan, Nanocomposites, Ionic gelation technique, Physico-Chemical Profile

1. Introduction
Chitosan is most abundant carbohydrate biopolymer in the world. Chitosan is a linear polysaccharide made up of randomly distributed α-(1-4)-linked D-glucosamine (deacetylated unit), produced commercially by deacetylation of chitin, which is the structural element in the exoskeleton of crustaceans (such as crabs and shrimp) and cell walls of fungi. Chitosan have special unique properties such as high surface area, adsorption properties, viscosity, soluble in various media, positive charge, basic polysaccharide, non-antigenicity, ideal candidate for bio-fabrication, polyelectrolyte behavior, ability to form films, metal chelation etc. Chitosan and its derivatives are attracted considerable interest among the agricultural researchers due to their biocompatibility, antimicrobial nature, environmentally safer (nontoxic) and biodegradability [1].

Among the various nanomaterials, metal based nanoparticles have been intensely used in agriculture as manifested by accumulation of publications [2-6]. But, the reports of phytotoxicity of metal nanomaterials have raised conscientious situation [7-12].

Recent advancements in synthesis of various nanomaterials of different sizes, shapes and functions establish nanotechnology as an indispensable technology for agriculture [11, 13]. Materials which show unique properties linked to their size (ranging from 1-1000 nm at least in one dimension) are considered nanoparticles and deemed under nanotechnology [14].

Various chitosan based nanoparticles were developed and amongst them Cu-chitosan nanoparticles expressed significant antifungal activity [15]. Although copper has traditionally been used as a major component of fungicides in agriculture but with increasing use at high dose, its level has exceeded the recommended limit of heavy metals in soil. Therefore, newer strategies need to be executed to overcome the problems of high dose of fungicides and to regulate the copper run-off. It is need of the hour to standardize a reproducible method of Cu-chitosan nanocomposite (NCP) synthesis and comprehensively evaluate its physico-chemical properties. The objective of this study was to solve the problem of preparation of Cu-chitosan NCPs with high degree of monodispersity and stability and investigate the effect of various parameters on the release profile of metal elements in Cu-chitosan NCPs.

2. Materials and methods

2.1 Synthesis of Cu-Chitosan NCPs

For synthesis of Cu-chitosan NCPs, a well established and reproducible method of cross linking coupled with ultra-sonication was used as described earlier [15-21]. 0.1 gm of chitosan (low molecular weight and 80% N-deacetylation, Sigma-Aldrich, St. Louis, USA) mixed in 100 ml of 1% acetic acid and stirrer at 500- 550 rpm for mixing (About 30 minutes). 0.25 gm of TPP (Sodium tripolyphosphate anhydrous, Loba Chemie) mix in 100 ml of deionized water and stirrer (Remi Laboratory Instruments, Mumbai, India) at 500- 550 rpm for mixing (About 30 minutes). Filter the solution using whatman qualitative filter paper-1. Then chitosan solution was stirrer at 500-550 rpm. TPP solution mixed in chitosan solution with dropping rate of about 40 drops/ minute (Fig.1). Both solutions obtained as a colloidal solution. Before finishing cross linking reaction as described above, $CuSO_4$ solution (0.02 gm in 10 ml) added into formulation and kept it for overnight stirring. The pellet resulting from centrifuge was suspended in deionized water by using ultra sonication with (Qsonica Missonix, USA) for 120 sec. at 4°C. It was repeated three times and the precipitated pellet was lyophilized (Freeze dryer with concentrator, Lab Tech) and stored at 4°C for further use.

Fig 1: Scale up synyhesis of Cu-chitosan Nanocomposites.

2.2 Characterization of Cu-chitosan NCPs

Developed Cu-chitosan NCPs were characterized for mean size, size distribution, functional group analysis and surface morphology by particle size analyzer (DLS: Dynamic Light Scattering), Fourier Transform Infra Red (FTIR), Transmission electron microscopy (TEM) and Scanning electron microscopy (SEM) through standardized methods [15, 20]. Elemental analysis of Cu-chitosan NCPs was gauged by energy dispersive spectroscopy (SEM-EDS).

2.2.1 Dynamic light scattering (DLS) measurements

DLS was used for measurement of average particle size, polydispersity index (PDI) and zeta potential of nanoparticles on high performance particle zetasizer (ZS90, *Malvern, UK*). The sample was analyzed in triplicate at 25ºC at a scattering angle of 90°. Deionized water was used as a reference for dispersing medium. The results are given as the average particle size obtained from the analysis of three different batches, each of them measured three times.

2.2.2 Fourier transforms infrared (FTIR) analysis

To confirm the synthesis of various nanoparticles, FTIR analysis was done. The results were recorded by ALPHA FT-IR spectrometer combined with Quick Snap™ (Bruker, Germany). FTIR spectroscopy is based on the chemical bonds in a molecule that vibrate at characteristic frequencies depending on the elements and types of bonds. During FTIR measurements, a spot on the specimen is subjected to a modulated IR beam. The specimen's transmittance and reflectance of the infrared radiation at different frequencies is measured and translated into an IR absorption plot.

2.2.3 Transmission electron microscopy (TEM)

In TEM, the nanocomposites were first diluted in ultrapure water (0.05 mg / ml, w/v), after which a negative staining technique was applied [22]. In this technique, the diluted suspension was mixed with 2% uranyl acetate solution; a drop of the mixture was deposited onto a standard copper grid covered by a holey carbon film and dried at ambient temperature before observation. TEM micrographs were obtained using a FEI Spirit TEM (Hillsboro, USA) operated at 120 kV using 400-mesh Formvar® carbon-coated copper grid.

2.2.4 Scanning electron microscopy (SEM) and energy dispersive X-ray spectroscope (EDS) observation

Scanning electron microscope was used to study the surface morphology of Cu-chitosan NCPs. The samples were dried by critical point drying (CPD, *Emitech* K850) and mounted on aluminium stubs with double sided carbon and then coated with gold palladium using a sputter coater model SC7620 (*Emitech*). The images were then recorded in high vacuum mode using a Zeiss EVO MA10 scanning electron microscope (*Carl Zeiss Promenade*, Jena, Germany) between 400 X – 29.70 KX magnification at 20 kV EHT [23]. Elemental analysis of nanoparticles were carried out by Zeiss EVOMA10 scanning electron microscope equipped with energy dispersive X-ray spectroscope elementary analyzer (EDS, *Oxford* Instruments) using analytical software QUANTAX 200.

2.3 Release Profile of Metal Elements in Cu-chitosan NCPs

Cu-encapsulation in Cu-chitosan NCP was analyzed under varying pH, agitation period and agitation rate [24]. Amount of copper ions encapsulated into chitosan NCPs was determined by double beam Atomic Absorption Spectroscopy (AAS4141 model, *Electronics Corporation of India Ltd*, India using following formula-

Concentration of embedded Cu in chitosan nanoparticles = Total Cu utilized in reaction – Free Cu in supernatant.

3. Results

3.1 Synthesis of Cu-Chitosan NCPs

Cu-chitosan NCP was prepared by interaction of TPP anion with cationic chitosan and further chelating of copper ions using ionic gelation method [20, 24]. Chitosan has inter and intra-molecular hydrogen bonding. Chitosan molecules in aqueous adopt extensive flexible structures due to the electrostatic repulsion between the chains. In diluted acetic acid, chitosan and TPP spontaneously formed dense micro-nano complex. Under specific intensity of ultrasonic waves, cavitations generated by ultrasonication reorganize the complex and

convert the micro complex into nano complex. Cu-chitosan NCP prepared in the present study exhibit a white crystal powder and appeared a semi transparent colloidal in aqueous.

3.2 Characterization of Cu-chitosan NCPs

DLS was used for the measurement of mean particles size, polydispersity index (PDI) and zeta potential of Cu-chitosan NCP. The size distribution profile, shown in Fig. 2A, represents mean hydrodynamic diameter of Cu-chitosan NCP, 295.4 ± 2.8nm. The PDI value 0.28 indicated monodisperse nature of Cu-chitosan NCP. Zeta potential of Cu-chitosan NCP (+ 19.6 mV, Fig. 2B) showed overall positive charge, which is important parameter for the stability and higher affinity towards biological membranes [15-17, 20].

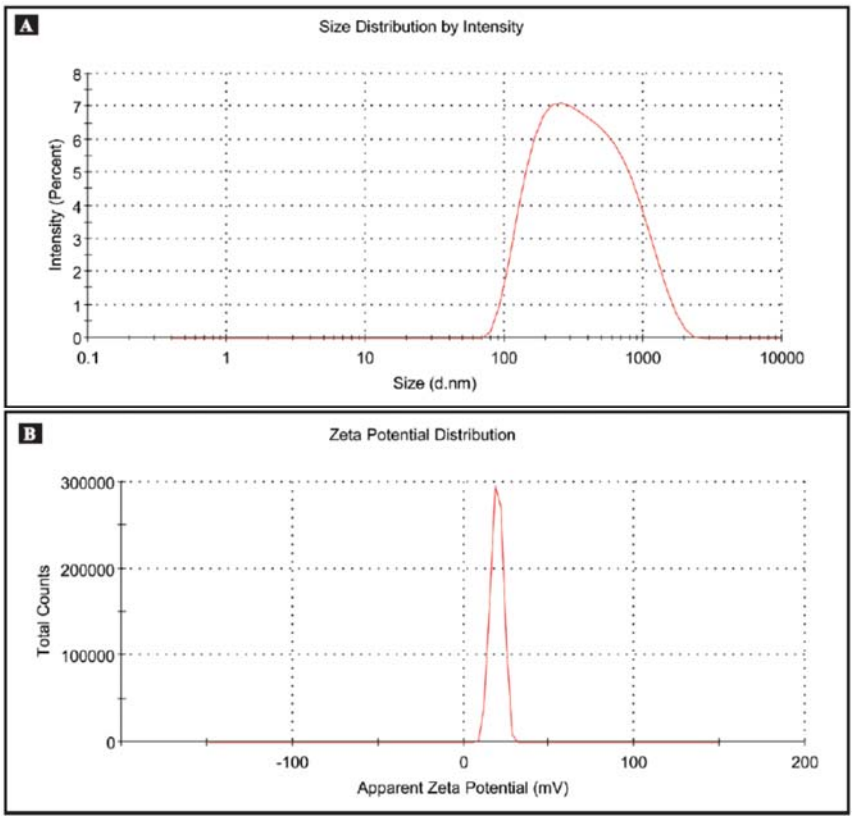

Fig 2: DLS analysis of Cu-chitosan NCPs (A) Size distribution by intensity and (B) Zeta potential distribution

3.2.1 Fourier Transforms Infrared (FTIR) Analysis

FTIR analysis was performed to confirm the interaction of chitosan, TPP and Cu. In bulk chitosan a specific peak at 3424 cm^{-1} corresponds to the combined peaks of the -NH_2 and -OH group stretching vibration. The band at 1647cm^{-1} is attributed to the CO-NH_2 group. The 1597 cm^{-1} peak of the -NH_2 bending vibration is sharper than the peak at 1647 cm^{-1}, which shows the high degree of deacetylation of the chitosan (Fig. 3A). The peaks at 1647 cm^{-1} (-$CONH_2$) and 1597 cm^{-1} (-NH_2) in the spectrum of Cu - chitosan NCP was sharper and shifted to 1643 and 1539 cm^{-1}. Therefore, Cu interaction with chitosan induces redistribution of vibration frequencies (Fig. 3B).

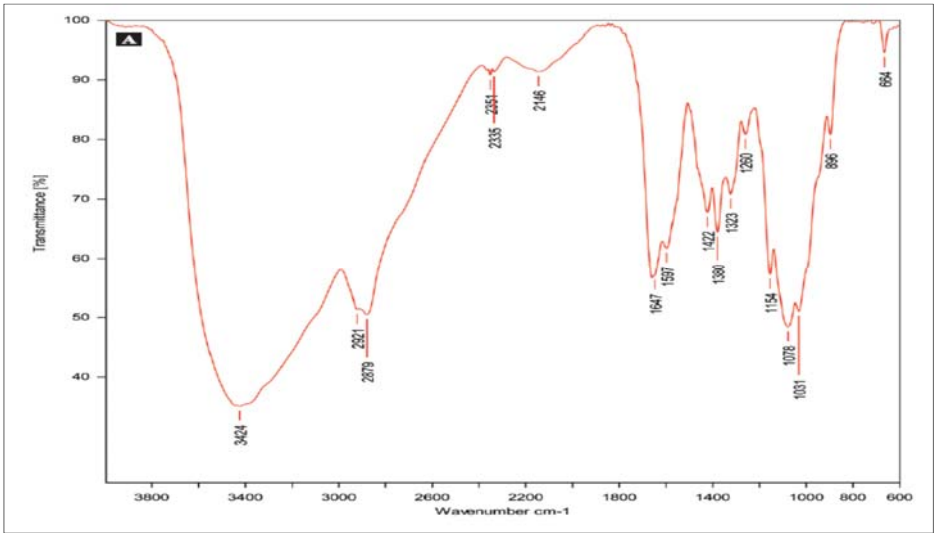

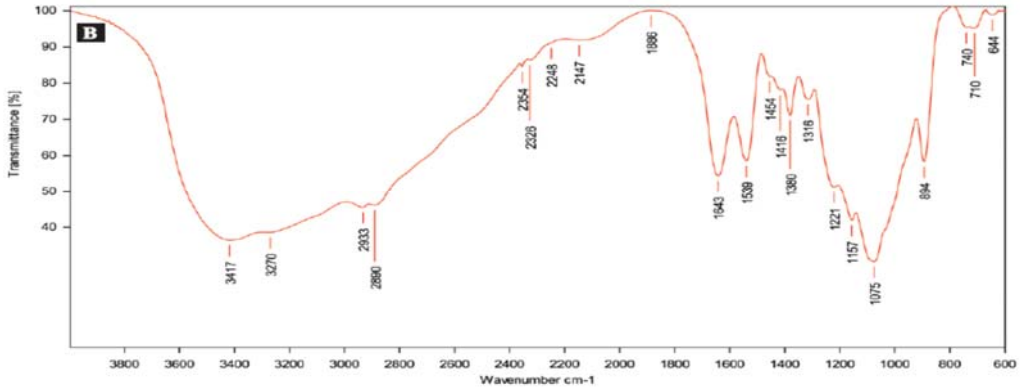

Fig 3: FTIR spectra (A) Bulk chitosan and (B) Cu-chitosan NCPs

3.2.2 TEM and SEM Analyses

Actual behaviour of nanoparticles in aqueous suspension comes only through TEM study. Sphere-shaped (Fig. 4A) NCP along with network of pores (Fig. 4B) verified by TEM. Further nano-organization of Cu-chitosan NCP was confirmed by SEM micrograph. Cu-chitosan NCP possesses homogenous crystalline morphology at lower magnification (Fig. 5A). Whereas, highly porous structure (like barred enclosure) was displayed at higher magnification. Micro and nanoscale size pores were observed as per SEM micrograph (Fig. 5B).

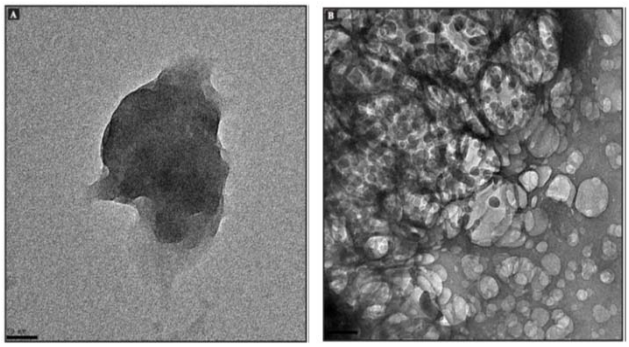

Fig 4: TEM images of (A) Sphere shaped Cu-chitosan NCPs and (B) Porous Cu-chitosan NCPs.

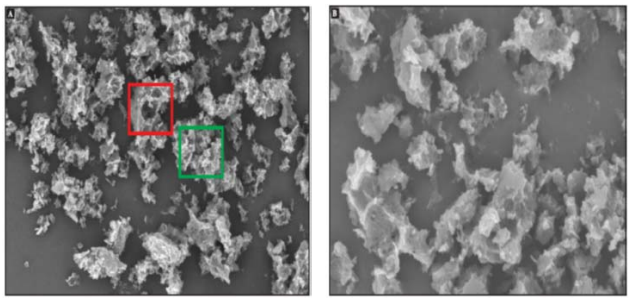

Fig 5: SEM micrographs (A) Cu-chitosan NCPs at 9.2mm ×1.00K and (B) Porous Cu-chitosan at 9.2mm ×3.00K revealed nano (in green rectangular) and micro size pores (in red rectangular)

3.2.3 SEM-Energy Dispersive X-ray Spectroscopy (EDS) Analysis

In addition to SEM, energy-dispersive X-ray spectroscopies (EDS) of different spots on the samples were taken for determining the elemental composition of Cu-chitosan NCP. Energy dispersive X-ray spectroscopy analysis revealed the presence of chitosan+ TPP (as C, O, P and N) and Cu in the NCP (Fig. 6A and B; Table 1). EDS analysis at porous surface of Cu-chitosan NCP as shown more Cu deposition compared to spectra of non porous surface. EDS study confirmed the presence of chitosan and Cu in the prepared NCP.

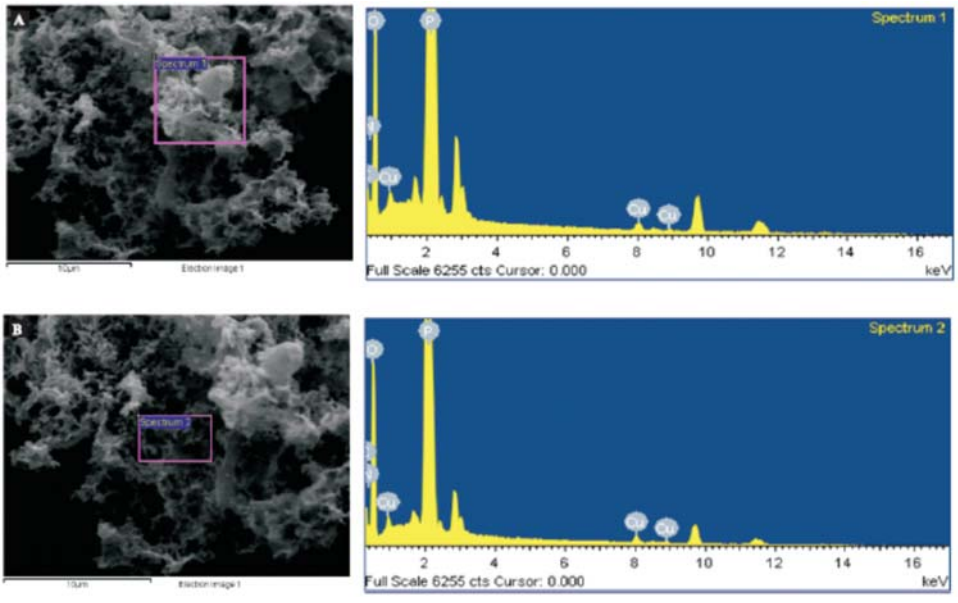

Fig 6: SEM-EDS elemental analysis of Cu-chitosan NCPs (A) Spectra of non-porous surface and (B) porous surface

Table 1: Elemental analysis of Cu-chitosan NCP

Elements	At porous spot		At non porous spot	
	Weight %	Atomic %	Weight %	Atomic %
C	54.43	63.02	43.75	52.78
O	30.19	26.24	35.15	31.83
P	6.19	2.78	9.8	4.58
N	7.69	7.63	10.20	10.55
Cu	1.51	0.33	1.09	0.25
Totals	100.00			

3.3 Release Profile of Metal Elements in Cu-chitosan NCP by Atomic Absorption Spectroscopy (AAS) Under Varying pH, Agitation Period and Agitation Rate

3.3.1 Effect of pH

Cu was encapsulated in increasing order (12, 44.3, 67.02 and 90.86%) from pH 1- 4. Further Cu encapsulation was decreased at pH 5 and 6 compared to pH 4 (Fig. 7A).

3.3.2 Effect of agitation period

Cu encapsulation in Cu-chitosan NCP was studied at various agitation periods *viz.* 20, 40, 60, 80 and 100 min. Maximum Cu was encapsulated at 40 min. (96.8%) and minimum encapsulation was at 20 min. (96.8%) (Fig.7B).

3.3.3 Effect of agitation rate

Cu encapsulation in Cu-chitosan NCP was studied at various agitation rates *viz.* 200, 400, 600 and 800 rpm. Maximum encapsulation (97.2%) of Cu was reported at 200 rpm and minimum (64.2%) encapsulation was at 400 rpm (Fig. 7C).

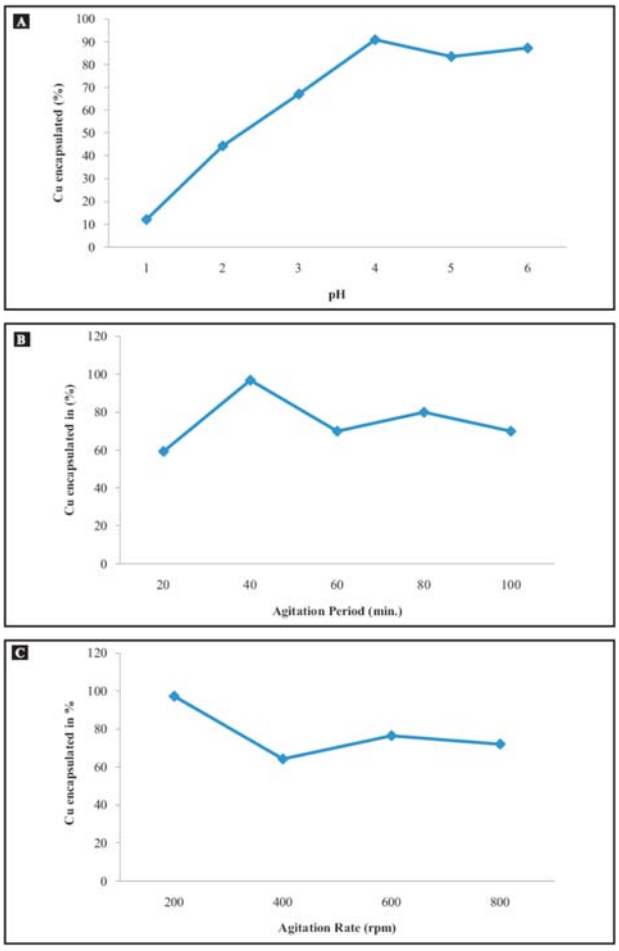

Fig 7: Cu- encapsulation in Cu-chitosan NCPs under varying (A) pH (B) Agitation period (C) Agitation rate.

4. Discussion

Cu-chitosan NCPs were prepared by the interaction of oppositely charged macromolecules (chitosan and TPP) using ionic gelation method [15-21]. In present study, mean hydrodynamic diameter of Cu-chitosan NCPs was 295.4 nm. The lower PDI value (0.28) specified the monodisperse nature of Cu-chitosan NCP. In present study, + 19.6 mV zeta potential was recorded, which indicate overall positive charge on the surface of NCPs. The positive zeta potential significantly influences particle stability in suspension through the electrostatic repulsion between the positively charged nanoparticles. Thus the nanoparticles remain separated in the suspension and formulation become stable. In addition, positively charged nanoparticles have more affinity towards the negatively charged biological membranes. Therefore nanoparticles express more biological interaction in living system. It also signifies for more antimicrobial activities [15-17, 20]. Charged nanoparticles have been reported to induce the foundation of new and longer pore by interacting with negatively charged macromolecules of biological membranes of fungi and bacteria, thus act as strong antimicrobial agents.

FTIR spectroscopy used infra-red waves which induce vibration in the chemical bonds and due to this vibration the presence and absence of functional group in sample could be examined. In present study, FTIR analysis was performed to confirm the interaction of chitosan, TPP and Cu. In bulk chitosan specific peaks at 3424 cm^{-1} and 1647cm^{-1}corresponds to the combined peaks of the $-NH_2$, -OH group stretching vibration and $CO-NH_2$ group were observed. In Cu - chitosan NCP spectrum, the peaks at 1647 cm^{-1} ($-CONH_2$) and 1597 cm^{-1} ($-NH_2$) were sharper and shifted to 1643 and 1539 cm^{-1}. Therefore, FTIR study showed redistribution of vibration frequencies in Cu-chitosan NCP in compared to bulk chitosan and these results were in line with earlier findings [15, 20]. TEM micrograph confirmed the nano-orgnization of synthesized materials. Spherical shaped Cu-chitosan NCP in range of 100-500 nm was observed under TEM study. TEM results obtained in present study, was found similar to earlier report, where Cu-chitosan NCP showed highly porous network of chitosan nanomaterials [20]. In present study SEM micrograph of Cu-chitosan NCP elucidate well organized spongy porous surface at 9.2mm ×1.00K [24]. Presence of Cu in chitosan NCP was confirmed by SEM-EDS. EDS spectra at porous and non porous surface of chitosan NCPs manifest higher and lower Cu deposition. In present study EDS spectrum undoubtedly explain the mechanism described earlier, in which Cu sorption could be understand by ion-exchange resins and surface chelating into porous nanomaterials [16].

Size, shape and stability of chitosan based nanoparticles mainly depend on pH, rate of agitation and agitation period [19]. In present study release profile of metal elements in Cu-chitosan NCP was studied under varying pH, agitation period and agitation rate by atomic absorption spectroscopy (AAS). Maximum Cu was encapsulated at pH 4 (90.86) and minimum encapsulation was at pH 1 (12%) in present study. Cu was encapsulated in increasing order with increasing pH. Therefore, Cu encapsulation efficiency was further decreased at pH 5 and 6. At low pH, amine groups easily form protonation which induce an electrostatic repulsion of Cu ions. Therefore, competition existed between protons and Cu ions for adsorption sites and adsorption capacity was decreased. At higher pH values, precipitation of Cu hydroxide occurs concurrently with the adsorption of Cu ions [25]. Cu encapsulation was also studied at various agitation periods

and agitation rate. Maximum Cu was encapsulated at 40 minutes (96.8%) of agitation period and 200 rpm (97.2%) of agitation rate. This may be due to the fact that at the start all adsorbent sites were available and later the absorption sites were decreased significantly [25-26]. It has been proved in present study that ionic gelation method of Cu-chitosan NCPs synthesis could be exploited for scale up process of nanoparticle production and further improvement could be performed in the NCPs by changing various factors in ionic gelation process.

5. Acknowledgments

Authors appreciate Nano Research Facility (NRF), Washington University in St. Louis for TEM analysis. Authors also acknowledge SEMF, Division of Entomology, IARI, New Delhi and SICART, Vallabh Vidyanagar, Anand, Gujarat for SEM analysis.

6. References

1. Choudhary MK, Kumara Swamy RV, Saharan V. Novel prospective for chitosan based nanomaterials in precision agriculture- a review. The bioscan. 2017; 12(1):155-159.
2. Oh SD, Lee S, Choi SH, Lee IS, Lee YM, Chun JH. *et al*. Synthesis of Ag and Ag-SiO_2 nanoparticles by γ-irradiation and their antibacterial and antifungal efficiency against *Salmonella enterica* serovar *Typhimurium* and *Botrytis* cinerea. Colloid and Surfaces A: Physicochemical and Engineering Aspects. 2006; 275:228-233.
3. Park HJ, Kim SH, Kim HJ, Choi SH. A new composition of nanosized silica-silver for control of various plant diseases. Plant Pathology Journal. 2006; 22:295-302.
4. Singh M, Singh S, Prasad S, Gambhir IS. Nanotechnology in medicine and antibacterial effect of silver nanoparticles. Digest Journal of Nanomaterials and Biostructures. 2008; 3:115-122.
5. Panacek A, Kolar M, Vecerova R, Prucek R, Soukupova J, Krystof V, *et al*. Antifugal activity of silver nanoparticles against *Candida spp.* Biomaterials. 2009; 30:6333-6340.
6. Nair R, Varghese SH, Nair BG, Maekawa T, Yoshida Y, Sakthi Kumar D. Nanoparticulate material delivery to plants. Plant Sciences. 2010; 179:154-163.
7. Lin D, Xing B. Root uptake and phytotoxicity of ZnO nanoparticles. Environmental Science & Technology. 2008; 42:5580-5582.
8. Kumari M, Mukherjee A, Chandrasekaran N. Genotoxicity of silver nanoparticles in *Allium cepa.* Science of the Total Environment. 2009; 407:5243-5246.
9. Sharon M, Choudhary A, Kumar R. Nanotechnology in agricultural diseases and food safety. Journal of Phytology. 2010; 2:83-92.
10. Dimkpa CO, McLean JE, Latta DE, Manango´n E, Britt DW, Johnson WP *et al*. Nanoparticles: phytotoxicity, metal speciation and induction of oxidative stress in sand-grown wheat. Journal of Nanoparticle Research. 2012; 14:11-25.
11. Khot L. Sankaran S, Maja J, Ehsani R, Schuster EW. Application of nanomaterial in agricultural production and crop production: A review. Crop Protection. 2012; 35:64-70.
12. Kah M, Hofmann T. Nanopesticide research: Current trends and future priorities. Environment International. 2014; 63:224-235.
13. Saharan V, Khatik R, Choudhary MK, Mehrotra A, Jakhar S, Raliya R, *et al*. Nano-materials for plant protection with special reference to Nano chitosan, In: proceedings of 4th Annual International conference on Advances in Biotechnology, GSTF, Dubai. 2014, 23-25.
14. Buzea CPI, Robbie K. Nanomaterials and nanoparticles: Sources and toxicity. Biointerphases. 2007; 2(4):17-71.
15. Saharan V, Mehrotra A, Khatik R, Rawal P, Sharma SS, Pal A. Synthesis of chitosan based nanoparticles and their *in vitro* evaluation against phytopathogenic fungi. International Journal of Biological Macromolecules. 2013; 62:677-683.
16. Qi L, Xu Z, Jiang X, Hu C, Zou X. Preparation and antibacterial activity of chitosan nanoparticles. Carbohydrate Research. 2004; 339(16):2693-2700.
17. Du WL, Niu SS, Xu YL, Xu ZR, Fan CL. Antibacterial activity of chitosan tripolyphosphate nanoparticles loaded with various metal ions. Carbohydrate Polymers. 2009; 75:385-389.
18. Corradini E, de Moura MR, Mattoso LHC. A preliminary study of the incorporation of NPK fertilizer into chitosan nanoparticles. eXPRESS Polymer Letters. 2010; 4(8):509-515.
19. Fan W, Yan W, Xu Z, Ni H. Formation mechanism of monodisperse, low molecular weight chitosan nanoparticles by ionic gelation technique. Colloids and Surfaces B: Biointerfaces. 2012; 90:21-27.
20. Saharan V, Sharma G, Yadav M, Choudhary MK, Sharma SS, Pal A, *et al.* Synthesis and *in vitro* antifungal efficacy of Cu–chitosan nanoparticles against pathogenic fungi of tomato. International Journal of Biological Macromolecules. 2015; 75:346-353.
21. Manikandan A, Sathiyabama M. Preparation of Chitosan nanoparticles and its effect on detached rice leaves infected with *Pyricularia grisea*. International Journal of Biological Macromolecules. 2016; 84:58-61.
22. Ottaviani MF, Favuzza P, Bigazzi M, Turro NJ, Jockusch S, Tomalia DA. A TEM and EPR investigation of the competitive binding of uranyl ions to starburst dendrimers and liposomes: potential use of dendrimers as uranyl ion sponges. Langmuir Journal. 2000; 16:7368-7372.
23. Rejinold SN, Muthunarayanan M, Muthuchelian K, Chennazhi KP, Nair SV, Jayakumar R. Saponin-loaded chitosan nanoparticles and their cytotoxicity to cancer cell lines *in vitro*. Carbohydrate Polymers. 2011; 84:407-416.
24. Jaiswal M, Chauhan D, Sankararama Krishnan N. Copper chitosan nanocomposite: synthesis, characterization, and application in removal of organophosphorous pesticide from agricultural runoff. Environmental Science Pollution Research. 2012; 19:2055-2062.
25. Wan Ngah WS, Endud CS, Mayanar R. Removal of copper (II) ions from aqueous solution onto chitosan and cross-linked chitosan beads. Reactive & Functional Polymers. 2002; 50:181-190.
26. Farghali AA, Bahgat M, Enaiet Allah A, Khedr MH. Adsorption of Pb (II) ions from aqueous solutions using copper oxide nanostructures. Beni-suef university journal of basic and applied sciences. 2013; 2:61-71.